Photoinduced pairing in Mott insulators

Satoshi Ejima[1,2⋆] **and Holger Fehske**[1,3]

1 Institut für Physik, Universität Greifswald, 17489 Greifswald, Germany
2 Institut für Softwaretechnologie, Abteilung High-Performance Computing, Deutsches Zentrum für Luft- und Raumfahrt (DLR), 22529 Hamburg, Germany
3 Erlangen National High Performance Computing Center, Friedrich-Alexander-Universität Erlangen-Nürnberg, 91058 Erlangen, Germany

⋆ satoshi.ejima@dlr.de

International Conference on Strongly Correlated Electron Systems (SCES 2022)
Amsterdam, 24-29 July 2022
doi:10.21468/SciPostPhysProc.11

Abstract

Utilizing time-evolution techniques in (infinite) matrix-product-state representation, we study the non-equilibrium dynamics of driven Mott insulators and demonstrate photoinduced η pairing directly in the thermodynamic limit. Analyzing the time evolution of the corresponding pairing correlations, we determine the optimal laser pump parameters for which long-range η-pairing becomes dominant after pulse irradiation. The time-dependent photoemission spectra for this optimal pump parameter set show clear signatures of the photoinduced insulator-to-metal phase transition related to the formation of η pairs.

Received 02-08-2022
Accepted 25-04-2023
Published 05-06-2023
doi:10.21468/SciPostPhysProc.11.009

1 Introduction

η pairing, proposed first by C. N. Yang in 1989 [1], gives rise to a pairing-density-wave-like off-diagonal long-range order in the Hubbard model. While it can be used to construct exact eigenstates of this model, η pairing is absent in the Hubbard model's ground state, and therefore has attracted only specific attention, mostly from mathematical point of view. Recently, however, it was pointed out that the η-pairing state will be enforced by pulse irradiation [2]. The respective enhancement of pairing correlations emerged in time-dependent exact diagonalisations: Calculating all eigenstates as well as pairing correlations for a small cluster and taking the selection rule of η pairs into account, Kaneko et al. showed that this photoinduced state is related to the η-pairing state [2].

Meanwhile, as a result of on-going developments in (time-depenent) density-matrix renormalisation group [(t-)DMRG] technique [3,4], optically driven systems in (quasi-)one-dimension can be simulated directly in the thermodynamic limit. In doing so, static correlation functions such as η-pair correlations can be computed by means of the infinite time-evolving block decimation (iTEBD) technique [5], taking advantage of translational invariance in the infinite matrix-product-state (iMPS) representation. Building window sites with so-called infinite boundary conditions (IBC) in the uniform update scheme [6] enables us to simulate non-equilibrium dynamics of excited (quasi-)one-dimensional (1D) systems by a laser electric field [7].

On this basis, in this study, we reexamine the time-evolution of photoinduced η-pairing, mainly to confirm or put in question previous small cluster results. Thereby we emphasize the importance of using optimal pump pulse parameters. Furthermore, we reconsider the relation between the η-pairing correlations and the optical spectrum in the small-amplitude regime after pulse irradiation. Finally we prove the photoinduced insulator-to-metal phase transition by simulating time-dependent photoemission spectra of driven Mott insulators.

2 Model

Let us consider the 1D half-filled Hubbard model,

$$\hat{H} = -t_{\mathrm{h}} \sum_{j,\sigma} \left(\hat{c}^{\dagger}_{j,\sigma} \hat{c}_{j+1,\sigma} + \mathrm{H.c.} \right) + U \sum_{j} \left(\hat{n}_{j,\uparrow} - 1/2 \right) \left(\hat{n}_{j,\downarrow} - 1/2 \right) , \tag{1}$$

where t_{h} is the nearest-neighbor transfer amplitude and U gives the on-site part of the Coulomb interaction. In Eq. (1), $\hat{c}^{\dagger}_{j,\sigma}$ ($\hat{c}_{j,\sigma}$) creates (annihilates) a spin-σ ($=\uparrow,\downarrow$) electron at Wannier lattice site j, and $\hat{n}_{j,\sigma} = \hat{c}^{\dagger}_{j,\sigma} \hat{c}_{j,\sigma}$. In the repulsive case ($U > 0$) the model realizes a Mott insulating ground state with a finite charge gap Δ.

Exact eigenstates of the Hubbard model can be constructed by means of the operators $\hat{\eta}^{+} = \sum_j (-1)^j \hat{\Delta}^{\dagger}_j$, $\hat{\eta}^{-} = (\hat{\eta}^{+})^{\dagger}$, and $\hat{\eta}^{z} = \frac{1}{2} \sum_j (\hat{n}_{j,\uparrow} + \hat{n}_{j,\downarrow} - 1)$, where $\hat{\Delta}^{\dagger}_j = \hat{c}^{\dagger}_{j,\downarrow} \hat{c}^{\dagger}_{j,\uparrow}$ denotes the singlet pair-creation operator [1]. These so-called η operators fulfill SU(2) commutation relations $[\hat{\eta}^{+}, \hat{\eta}^{-}] = 2\hat{\eta}^{z}$ and $[\hat{\eta}^{z}, \hat{\eta}^{\pm}] = \pm \hat{\eta}^{\pm}$. Apparently, the Hubbard Hamiltonian (1) commutes with $\hat{\eta}^2 = \frac{1}{2}(\hat{\eta}^{+}\hat{\eta}^{-} + \hat{\eta}^{-}\hat{\eta}^{+}) + (\hat{\eta}^{z})^2$, i.e., $\langle \eta^2 \rangle$ is a conserved quantity. Long-ranged pairing correlations $\langle \hat{\eta}^{+}_j \hat{\eta}^{-}_{\ell} \rangle$ develop when the expectation value $\langle \hat{\eta}^2 \rangle$ becomes finite, but such η-pairing states cannot be the ground state of the Hubbard model [1]. Pulse irradiation can establish η-paired states in Mott insulators however [2].

To address this issue, we apply a pump pulse with amplitude A_0, frequency ω_{p} and width σ_{p}, centered at time $t_0 (> 0)$:

$$A(t) = A_0 e^{-(t-t_0)^2/(2\sigma_{\mathrm{p}}^2)} \cos\left[\omega_{\mathrm{p}} (t - t_0) \right] . \tag{2}$$

The external time-dependent electric field $A(t)$ changes the hopping amplitude by a Peierls phase [8]: $t_{\mathrm{h}} \hat{c}^{\dagger}_{j,\sigma} \hat{c}_{j+1,\sigma} \to t_{\mathrm{h}} e^{\mathrm{i}A(t)} \hat{c}^{\dagger}_{j,\sigma} \hat{c}_{j+1,\sigma}$, i.e., $\hat{H} \to \hat{H}(t)$. As a result, the system being initially in the ground state, is driven out of equilibrium, $|\psi(0)\rangle \to |\psi(t)\rangle$.

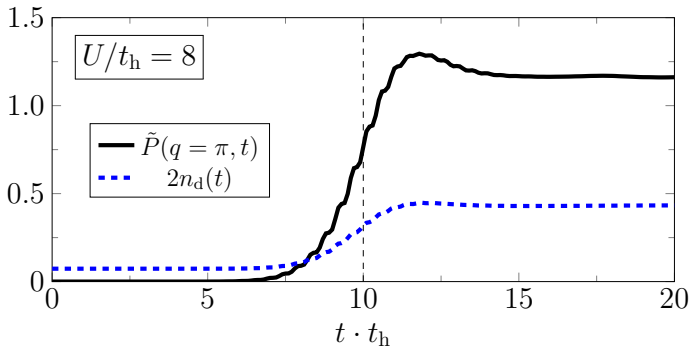

Figure 1: Typical time-evolution process of $\tilde{P}(q = \pi, t)$ and $2n_\mathrm{d}(t)$ for the photoinduced η-pairing states in the strong-coupling regime of the driven Hubbard model with $U/t_\mathrm{h} = 8$ and pump parameters A_0=0.4, $\omega_\mathrm{p}/t_\mathrm{h} = 7.0$, $\sigma_\mathrm{p} = 2t_\mathrm{h}^{-1}$ and $t_0 = 10t_\mathrm{h}^{-1}$. The iTEBD data are obtained for bond dimension $\chi = 1200$, ensuring a truncation error smaller than 10^{-5}. For the iTEBD calculations, we employ a second-order Suzuki-Trotter decomposition with time step $0.1t_\mathrm{h}^{-1}$ ($0.01t_\mathrm{h}^{-1}$).

3 Pairing correlations

The η-pairing state can be detected evaluating the time evolution of the pair-correlation function

$$P(r,t) = \frac{1}{L}\sum_j \langle\psi(t)|\hat{\Delta}^\dagger_{j+r}\hat{\Delta}_j + \text{H.c.})|\psi(t)\rangle\,, \tag{3}$$

and its Fourier transform $\tilde{P}(q,t) = \sum_r e^{\mathrm{i}qr}P(r,t)$. As found in Refs. [2, 9] for small clusters, $\tilde{P}(\pi,t)$ is enhanced after pulse irradiation, indicating the formation of an η-pairing state. By means of iTEBD this is confirmed directly in the thermodynamic limit which is demonstrated in Fig. 1 for a pump with $A_0 = 0.4$, $\omega_\mathrm{p}/t_\mathrm{h} = 7.0$ and $\sigma_\mathrm{p} = 2t_\mathrm{h}^{-1}$ centered at $t_0 = 10t_\mathrm{h}^{-1}$. $\tilde{P}(\pi,t)$ shows a clear response to pulse irradiation and is strengthened as the system progresses in time until saturation is reached. Obviously, the nonlocal contributions have a stronger impact on $\tilde{P}(\pi,t)$ than the double occupancy $n_\mathrm{d}(t) = (1/L)\sum_j\langle\psi(t)|\hat{n}_{j,\uparrow}\hat{n}_{j,\downarrow}|\psi(t)\rangle$ [note that $P(r=0,t) = 2n_\mathrm{d}(t)$, where $n_\mathrm{d}(0) > 0$ for the finite U values considered].

The enhancement process of η-pairing can be described as follows [2]: The initial state before pulse irradiation is the ground state of the Hubbard chain with $|\eta = 0, \eta^z = 0\rangle$, which is consistent with the numerical finding: $\tilde{P}(0, t = 0) \simeq 0$ (see Fig. 1). Turning on the pump pulse, the Hamiltonian does not commute with the η-operators anymore,

$$[\hat{H}(t), \eta^+] = [\hat{H}, \eta^+]\cos[A(t)] + \sum_k F(k,t)\hat{c}^\dagger_{\pi-k,\downarrow}\hat{c}^\dagger_{k,\uparrow}\,, \tag{4}$$

where $F(k,t) = 4t_\mathrm{h}\sin[A(t)]\sin k$. This alters the initial state to a state with a finite expectation value $\langle\hat{\eta}^2\rangle$. Even though the commutation relation is recovered for $t \gg t_0$, i.e., $[\hat{H}(t), \hat{\eta}^+] \to [\hat{H}, \hat{\eta}^+]$ [since $A(t) \to 0$], $|\psi(t)\rangle$ now includes components of $|\eta > 0, \eta^z = 0\rangle$ leading to the enhancement of $\tilde{P}(\pi,t)$, see Fig. 1 for $t > t_0$.

Note that the enhancement of η pairing after pulse irradiation depends strongly on the pump pulse parameters. The optimal parameter set for inducing η-pairing states can be determined examining the A_0 and ω_p dependences of $\tilde{P}(\pi,t)$ by iTEBD. Figure 2(a) shows the contour plot of $\tilde{P}(\pi,t)$ after pulse irradiation ($t = 15t_\mathrm{h}^{-1}$). We find a single maximum around $A_0 \approx 0.4$ and $\omega_\mathrm{p}/t_\mathrm{h} \approx 7.0$ (marked by the "×" symbol), instead of the stripe structure observed in the finite-system ($L = 14$) exact diagonalisation (ED) simulations [2].

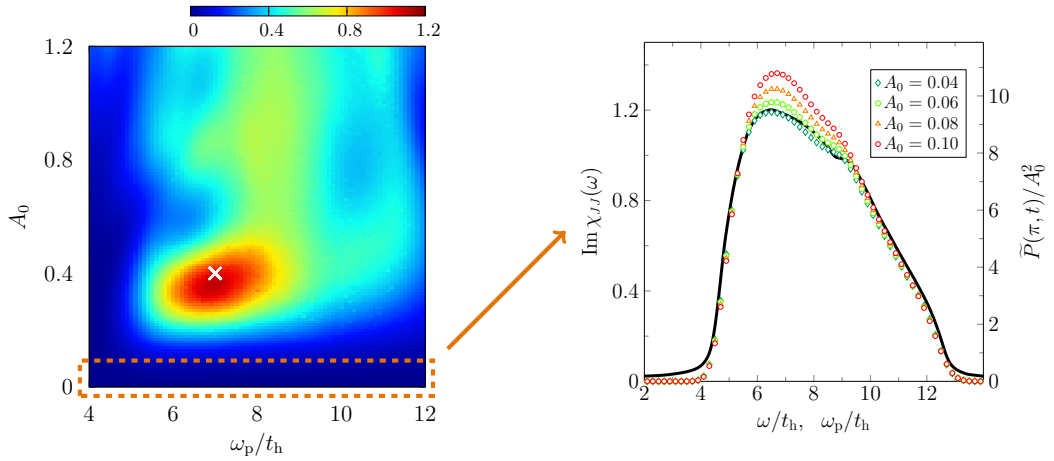

Figure 2: (a): Contour plots of $\tilde{P}(q=\pi,t)$ in the ω_p-A_0 plane at $t=15t_h^{-1}$. Again $U/t_h=8$, and the pump is parametrized by $\sigma_p=2t_h^{-1}$ at $t_0=10t_h^{-1}$. (b): $\tilde{P}(\pi,t)$ at $t=15t_h^{-1}$ in the small-A_0 area enclosed by the dashed square in panel (a). Dividing by A_0^2, data can be rescaled to $\mathrm{Im}\chi(\omega)$ (black line), where $\mathrm{Im}\chi(\omega)$ is the imaginary part of the optical spectrum $\chi_{JJ}(\omega)$.

Another notable results of previous ED calculations [2] was that the peak structure of $\tilde{P}(\pi,t)$ as a function of ω_p for small A_0 is essentially the same as those of the ground-state optical spectrum,

$$\chi_{JJ}(\omega>0)=-\frac{1}{L}\langle\psi_0|\hat{J}\frac{1}{E_0-\hat{H}+\hbar\omega+\mathrm{i}\eta_L}\hat{J}\,|\psi_0\rangle\,, \tag{5}$$

where $|\psi_0\rangle$ is the ground state having energy E_0 and Lorentzian width η_L. In (5), the Hubbard-model charge-current operator is $\hat{J}=\mathrm{i}t_h\sum_{j,\sigma}\left(\hat{c}^\dagger_{j,\sigma}\hat{c}_{j+1,\sigma}-\hat{c}^\dagger_{j+1,\sigma}\hat{c}_{j,\sigma}\right)$.

Figure 2(b) compares the iTEBD data, obtained for $\tilde{P}(\pi,t)$ at various small A_0 and $t=15t_h^{-1}$, with the t-DMRG results for $\chi_{JJ}(\omega)$ (using $\eta_L/t_h=0.2$), in dependence on ω_p respectively ω. Most notably, $\tilde{P}(\pi,t)$ divided by A_0^2 scales to the imaginary part of the optical spectrum $\mathrm{Im}\chi(\omega)$. This can be understood as follows: The hopping term including the Peierls phase can be divided into kinetic and current operators as

$$-t_h\sum_{j,\sigma}\left(e^{\mathrm{i}A(t)}\hat{c}^\dagger_{j,\sigma}\hat{c}_{j+1,\sigma}+\mathrm{H.c.}\right)=\hat{K}\cos[A(t)]+\hat{J}\sin[A(t)]\,, \tag{6}$$

where $\hat{K}=-t_h\sum_{j,\sigma}(\hat{c}^\dagger_{j,\sigma}\hat{c}_{j+1,\sigma}+\mathrm{H.c.})$. For small A_0 and large t, the second term in Eq. (6) can be approximated by $\hat{J}A_0$, yielding a significant contribution of A_0^2 to the pair correlations. Needless to say that the finite-size effects are eliminated by simulating the pair correlations directly in thermodynamic limit by iTEBD, leading to the single-peak structure in Fig. 2(b), in strong contrast to the multiple-peak structure observed in the ED calculations [2].

4 Non-equilibrium dynamics

We now analyze the non-equilibrium photoemission spectra $A(k,\omega;t)=\sum_{\sigma=\uparrow,\downarrow}A_\sigma(k,\omega;t)$ for the optimal pump parameter set marked by the "×"-symbol in Fig. 2(a). To explore the system

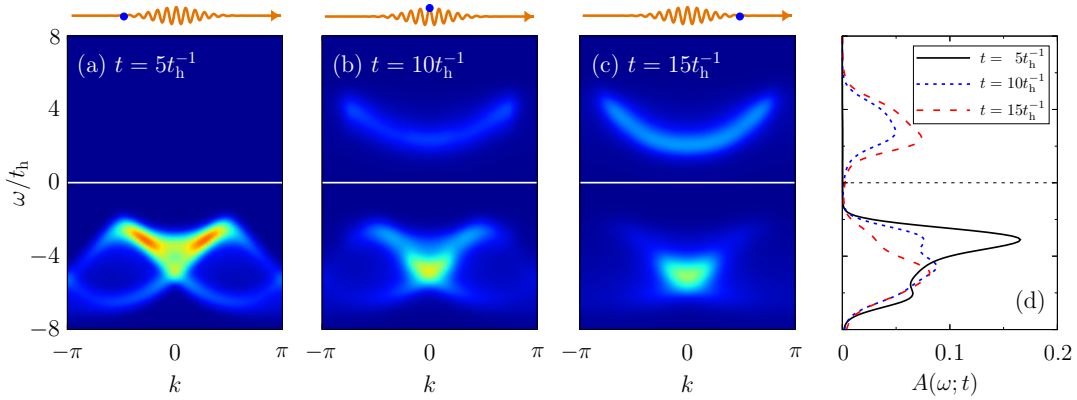

Figure 3: Snapshots of the photoemission spectra $A(k,\omega;t)$ indicating photoinduced η-pairing during the pump at times $t = 5t_h^{-1}$ (a), $10t_h^{-1}$ (b) and $15t_h^{-1}$ (c). The pump is parametrized by $A_0 = 0.4$, $\omega_p/t_h = 7.0$ [see '×'-symbol in Fig. 2(a)], and $\sigma_p = 2t_h^{-1}$ at $t_0 = 10t_h^{-1}$. The transient integrated density of states $A(\omega;t)$ obtained from the data of panels (a)-(c) is depicted in panel (d). All data are obtained by the (i)TEBD technique with IBC for the 1D half-filled Hubbard model with $U/t_h = 8$. Note that the time cutoff in the simulation of time-dependent correlation functions is $T = 5t_h^{-1}$, i.e., the integration in Eq. 7 extends only over the interval $-T \le \tau_1, \tau_2 \le T$. As a compromise between time and frequency resolutions we have chosen a probe pulse width $\sigma_{pr} = 2t_h^{-1}$.

dynamics in a non-equilibrium situation, time-dependent spectral functions of the form [10]

$$A_\sigma(k,\omega;t) = \sum_r e^{-ikr} \int_{-\infty}^{\infty}\int_{-\infty}^{\infty} d\tau_1 d\tau_2 f(\tau_1,\tau_2;\omega)\cdot C_\sigma(r,\tau_1,\tau_2;t) \tag{7}$$

are of interest. Here, the non-equilibrium two-point correlator

$$C_\sigma(r,\tau_1,\tau_2;t) = \langle\phi(t)|\hat{c}^\dagger_{j+r,\sigma}(\tau_1;t)\hat{c}_{j,\sigma}(\tau_2;t)|\phi(t)\rangle \tag{8}$$

defined relative to t is calculated not using the iMPS $|\psi(t)\rangle$ but the MPS $|\phi(t)\rangle$ with $L_W = 128$ window sites and IBC, and

$$f(\tau_1,\tau_2;\omega) = e^{i\omega(\tau_1-\tau_2)} g(\tau_1)g(\tau_2), \quad g(\tau) = \exp[-\tau^2/2\sigma_{pr}^2]/(\sqrt{2\pi}\sigma_{pr}) \tag{9}$$

specify the shape of the probe pulse, e.g., in a time-dependent photoemission spectroscopy experiment. How numerically simulate two-time-dependent quantities such as $C_\sigma(r,\tau_1,\tau_2;t)$ has been explained in detail in Ref. [7] [see paragraphs below Eq. (1)].

Figure 3 displays our (i)TEBD results for the 1D half-filled Hubbard model in the strong-coupling regime ($U/t_h = 8$). Before pump irradiation the state is a Mott insulator with a noticable single-particle gap, see Fig. 3(a) for $t = 5t_h^{-1}$. In the midst of the pump ($t = 10t_h^{-1}$), an extra dispersion above Fermi energy ($\omega > E_F$) appears and persists afterwards [Fig. 3(c)].

Evaluating the integrated density of states

$$A(\omega;t) = \frac{1}{L}\sum_k A(k,\omega;t), \tag{10}$$

we see more clearly how the spectral weight is shifted from $\omega < E_F$ to $\omega > E_F$ due to the photoinduced η-pairing. Figure 3(d) gives $A(\omega;t)$ for the photoinduced η-pairing state. Obviously, the spectral weight for $\omega > E_F$ increases distinctly over time, indicating a photoinduced phase transition from a Mott insulator to a metallic η-pairing state. This photoinduced

insulator-to-metal transition should be observed in time- and angle-resolved photoemission spectroscopy, when the pure Hubbard model is realized experimentally, e.g., in optical lattices. We note that the photoinduced phase transition cannot be observed by simulating the time-dependent photoemission spectra with not-optimized pump-pulse parameters, see Ref. [7].

5 Conclusions

To summarize, combining tensor-network algorithms with infinite time-evolving block decimation techniques, we revisited the problem of photoinducing η-pairing states in the one-dimensional Hubbard model at half band filling. This allowed us to prove the enhancement of the pairing correlations directly in the thermodynamic limit. We also determined the optimal pump-pulse parameter set that maximizes the η-pairing tendency. An η-pairing related Mott insulator to metal transition could be extracted from the time-dependent photoemission spectrum.

We wish to stress that the numerical approach presented here can be applied to simulate the non-equilibrium dynamics of any (quasi-)one-dimensional translational-invariant system in entire ranges of interacting and driving parameters. For example, the photoinduced metallization of excitonic insulators was demonstrated quite recently in accordance with time- and angle-resolved photoemission spectroscopy experiments on Ta_2NiSe_5 [14, 15].

Acknowledgements

The iTEBD simulations were performed using the ITensor library [16].

Funding information S.E. was supported by Deutsche Forschungsgemeinschaft through project EJ 7/2-1.

References

[1] C. N. Yang, *η pairing and off-diagonal long-range order in a Hubbard model*, Phys. Rev. Lett. **63**, 2144 (1989), doi:10.1103/PhysRevLett.63.2144.

[2] T. Kaneko, T. Shirakawa, S. Sorella and S. Yunoki, *Photoinduced η pairing in the Hubbard model*, Phys. Rev. Lett. **122**, 077002 (2019), doi:10.1103/PhysRevLett.122.077002.

[3] S. R. White, *Density matrix formulation for quantum renormalization groups*, Phys. Rev. Lett. **69**, 2863 (1992), doi:10.1103/PhysRevLett.69.2863.

[4] U. Schollwöck, *The density-matrix renormalization group in the age of matrix product states*, Ann. Phys. **326**, 96 (2011), doi:10.1016/j.aop.2010.09.012.

[5] G. Vidal, *Classical simulation of infinite-size quantum lattice systems in one spatial dimension*, Phys. Rev. Lett. **98**, 070201 (2007), doi:10.1103/PhysRevLett.98.070201.

[6] V. Zauner, M. Ganahl, H. G. Evertz and T. Nishino, *Time evolution within a comoving window: Scaling of signal fronts and magnetization plateaus after a local quench in quantum spin chains*, J. Phys. Condens. Matter **27**, 425602 (2015), doi:10.1088/0953-8984/27/42/425602.

[7] S. Ejima, F. Lange and H. Fehske, *Nonequilibrium dynamics in pumped Mott insulators*, Phys. Rev. Res. **4**, L012012 (2022), doi:10.1103/PhysRevResearch.4.L012012.

[8] R. Peierls, *Zur Theorie des Diamagnetismus von Leitungselektronen*, Z. Phys. **80**, 763 (1933), doi:10.1007/BF01342591.

[9] S. Ejima, T. Kaneko, F. Lange, S. Yunoki and H. Fehske, *Photoinduced η-pairing in one-dimensional Mott insulators*, JPS Conf. Proc. **30**, 011184 (2020), doi:10.7566/JPSCP.30.011184.

[10] J. K. Freericks, H. R. Krishnamurthy and T. Pruschke, *Theoretical description of time-resolved photoemission spectroscopy: Application to pump-probe experiments*, Phys. Rev. Lett. **102**, 136401 (2009), doi:10.1103/PhysRevLett.102.136401.

[11] G. Vidal, *Efficient classical simulation of slightly entangled quantum computations*, Phys. Rev. Lett. **91**, 147902 (2003), doi:10.1103/PhysRevLett.91.147902.

[12] F. Lange, S. Ejima and H. Fehske, *Finite-temperature dynamic structure factor of the spin-1 XXZ chain with single-ion anisotropy*, Phys. Rev. B **97**, 060403 (2018), doi:10.1103/PhysRevB.97.060403.

[13] S. Ejima, F. Lange and H. Fehske, *Finite-temperature photoemission in the extended Falicov-Kimball model: A case study for Ta_2NiSe_5*, SciPost Phys. **10**, 077 (2021), doi:10.21468/scipostphys.10.3.077.

[14] S. Ejima, F. Lange and H. Fehske, *Photoinduced metallization of excitonic insulators*, Phys. Rev. B **105**, 245126 (2022), doi:10.1103/PhysRevB.105.245126.

[15] K. Okazaki et al., *Photo-induced semimetallic states realised in electron-hole coupled insulators*, Nat. Commun. **9**, 4322 (2018), doi:10.1038/s41467-018-06801-1.

[16] M. Fishman, S. White and E. Stoudenmire, *The ITensor software library for tensor network calculations*, SciPost Phys. Codebases 4 (2022), doi:10.21468/SciPostPhysCodeb.4.